

# Phase Behavior of EVAL Polymers in Water-2-Propanol Cosolvent

Tai-Horng Young\*

Center for Biomedical Engineering, College of Medicine, National Taiwan University, Taipei, Taiwan, R.O.C.

Liao-Ping Cheng

Department of Chemical Engineering, Tamkang University, Taipei, Taiwan, R.O.C.

Chih-Chen Hsieh and Leo-Wang Chen

Department of Chemical Engineering, National Taiwan University, Taipei, Taiwan, R.O.C.

Received July 14, 1997; Revised Manuscript Received November 18, 1997

**ABSTRACT:** Isothermal phase diagrams for semicrystalline poly(ethylene-*co*-vinyl alcohol) (EVAL) using two nonsolvents (water and 2-propanol) serving as a cosolvent system have been determined. The locations of the liquid–liquid demixing and the crystallization-induced gelation in the phase diagrams at 60 °C were identified. Attempts were made to correlate the experimental findings with predictions on the basis of the modified Flory–Huggins theory for ternary solutions using three binary interaction parameters ( $\chi_{ij}$ ) and one ternary interaction parameter ( $\chi_T$ ). No good agreement was found between the theoretical predictions and experimentally obtained data if the ternary interaction parameter was neglected. But an improvement can be obtained when a ternary interaction parameter is considered. The optimum value has been found to be approximately  $-1.7 + 0.5\phi_2 + 1.0\phi_3$ . Therefore, it is necessary to introduce the ternary interaction parameter when the binary parameters provide an inadequate description of phase behavior, but in most systems studied so far the ternary interaction parameter is ignored.

## Introduction

Phase diagrams can provide valuable information on the importance of the various phase transitions that are responsible for the preparation of membranes by immersion of a polymer solution in a coagulation bath. Experimentally obtained liquid–liquid demixing and crystallization boundaries have been investigated for several polymers in solvent–nonsolvent mixtures. In this work, phase equilibria in the ternary system water, 2-propanol, and poly(ethylene-*co*-vinyl alcohol) (EVAL) were studied. EVAL is insoluble in either water or 2-propanol separately, but certain mixtures of water and 2-propanol dissolve the EVAL. Although the cosolvent event has been known for some time,<sup>1</sup> systematic studies of the complete phase behavior are very scarce.<sup>2,3</sup> Most attempts to analyze the phase behavior of ternary systems are based on a consideration of the binary interaction parameter embodied in the Flory–Huggins theory. However, a cosolvent system is described as one in which mixtures of two liquids dissolve a polymer that is insoluble in either liquid separately. This suggests that binary interaction parameters are not the controlling parameter in a cosolvent system and a ternary interaction parameter should have much greater significance. In addition, it is well-known that for an accurate description of the preferential sorption of polymers in mixed solvents, ternary interaction parameters are required.<sup>4,5</sup> In a like manner, a ternary interaction parameter is required for an accurate de-

scription of the thermodynamics of other ternary systems. This applies especially to a cosolvent system. Therefore, the question of whether a ternary interaction parameter is necessary is discussed in this work, through comparing theoretical predictions and experimentally obtained data for the phase behavior of EVAL in water–2-propanol cosolvents at 60 °C. The results indicate that in this system it is necessary to take into account the ternary interaction parameter. Some examples of the influence of the ternary interaction parameter on the liquid–liquid miscibility gap and solid–liquid miscibility gap are presented.

## Theory

In this study, the Flory–Huggins theory is used to describe the Gibbs free energy of mixing ( $\Delta G_m$ ) for ternary polymer solutions,<sup>6</sup> in which a ternary interaction parameter,  $\chi_T$ , is included:<sup>7</sup>

$$\Delta G_m = RT(n_1 \ln \phi_1 + n_2 \ln \phi_2 + n_3 \ln \phi_3 + \chi_{12}n_1\phi_2 + \chi_{13}n_1\phi_3 + \chi_{23}n_2\phi_3 + \chi_T n_1\phi_2\phi_3) \quad (1)$$

where  $n_i$  and  $\phi_i$  are the number of moles and volume fraction of component  $i$  ( $i = 1$ , water;  $i = 2$ , 2-propanol;  $i = 3$ , EVAL).  $\chi_{ij}$  are binary interaction parameters between component  $i$  and component  $j$ . From eq 1, the chemical potential,  $\Delta\mu_i$  ( $\mu_i - \mu_i^\circ$ ) of the three components is given

$$\begin{aligned} \frac{\Delta\mu_1}{RT} = & \ln \phi_1 + 1 - \phi_1 - \frac{V_1}{V_2}\phi_2 - \frac{V_1}{V_3}\phi_3 + \\ & (\phi_2\chi_{12} + \phi_3\chi_{13})(\phi_2 + \phi_3) - \frac{V_1}{V_2}\phi_2\phi_3\chi_{23} - \\ & h_1h_2\phi_2 \frac{d\chi_{12}}{dh_2} - \phi_1\phi_2\phi_3 \frac{\partial\chi_{13}}{\partial\phi_2} - \phi_1\phi_3^2 \frac{\partial\chi_{13}}{\partial\phi_2} - \phi_1\phi_3^2 \frac{\partial\chi_{13}}{\partial\phi_3} - \\ & \frac{V_1}{V_2}\phi_2^2\phi_3 \frac{\partial\chi_{23}}{\partial\phi_2} - \frac{V_1}{V_2}\phi_2\phi_3^2 \frac{\partial\chi_{23}}{\partial\phi_3} - \phi_1\phi_2^2\phi_3 \frac{\partial\chi_T}{\partial\phi_2} - \\ & \phi_1\phi_2\phi_3^2 \frac{\partial\chi_T}{\partial\phi_3} + \chi_T\phi_2\phi_3(1 - 2\phi_1) \quad (2) \end{aligned}$$

$$\begin{aligned} \frac{\Delta\mu_2}{RT} = & \ln \phi_2 + 1 - \phi_2 - \frac{V_2}{V_1}\phi_1 - \frac{V_2}{V_3}\phi_3 + \\ & \left( \frac{V_2}{V_1}\phi_1\chi_{12} + \phi_3\chi_{23} \right) (\phi_1 + \phi_3) - \frac{V_2}{V_1}\phi_1\phi_3\chi_{13} + \\ & \frac{V_2}{V_1}h_1h_2\phi_1 \frac{d\chi_{12}}{dh_2} + \frac{V_2}{V_1}\phi_1\phi_3(\phi_1 + \phi_3) \frac{\partial\chi_{13}}{\partial\phi_2} - \\ & \frac{V_2}{V_1}\phi_1\phi_3^2 \frac{\partial\chi_{13}}{\partial\phi_3} + \phi_2\phi_3(\phi_1 + \phi_3) \frac{\partial\chi_{23}}{\partial\phi_2} - \phi_2\phi_3^2 \frac{\partial\chi_{23}}{\partial\phi_3} + \\ & \frac{V_2}{V_1}\phi_1\phi_2\phi_3(\phi_1 + \phi_3) \frac{\partial\chi_T}{\partial\phi_2} - \frac{V_2}{V_1}\phi_1\phi_2\phi_3^2 \frac{\partial\chi_T}{\partial\phi_3} + \\ & \frac{V_2}{V_1}\chi_T\phi_1\phi_3(1 - 2\phi_2) \quad (3) \end{aligned}$$

$$\begin{aligned} \frac{\Delta\mu_3}{RT} = & \ln \phi_3 + 1 - \phi_3 - \frac{V_3}{V_1}\phi_1 - \frac{V_3}{V_2}\phi_2 + \\ & \left( \frac{V_3}{V_1}\phi_1\chi_{13} + \frac{V_3}{V_2}\phi_2\chi_{23} \right) (\phi_1 + \phi_2) - \frac{V_3}{V_1}\phi_1\phi_2\chi_{12} - \\ & \frac{V_3}{V_1}\phi_1\phi_2\phi_3 \frac{\partial\chi_{13}}{\partial\phi_2} - \frac{V_3}{V_2}\phi_2^2\phi_3 \frac{\partial\chi_{23}}{\partial\phi_2} + \\ & \phi_3(\phi_1 + \phi_2) \left[ \frac{V_3}{V_1}\phi_1 \frac{\partial\chi_{13}}{\partial\phi_3} + \frac{V_3}{V_2}\phi_2 \frac{\partial\chi_{23}}{\partial\phi_3} \right] - \\ & \frac{V_3}{V_1}\phi_1\phi_2^2\phi_3 \frac{\partial\chi_T}{\partial\phi_2} + \frac{V_3}{V_1}\phi_1\phi_2\phi_3(\phi_1 + \phi_2) \frac{\partial\chi_T}{\partial\phi_3} + \\ & \frac{V_3}{V_1}\chi_T\phi_1\phi_2(1 - 2\phi_3) \quad (4) \end{aligned}$$

where  $\mu_i^\circ$  is the chemical potential at standard state,  $V_i$  is the molar volume,  $h_1 = \phi_1/(\phi_1 + \phi_2)$ , and  $h_2 = \phi_2/(\phi_1 + \phi_2)$ .

**Liquid-Liquid Phase Equilibrium.** At equilibrium between two phases ( $\alpha$  and  $\beta$ ) in the ternary system at a specified temperature and pressure, the chemical potentials of each component in these two phases are equal, i.e.,

$$\mu_i^\alpha = \mu_i^\beta \quad i = 1-3 \quad (5)$$

where  $\mu_i^\alpha$  and  $\mu_i^\beta$  are the chemical potentials of component  $i$  in phases  $\alpha$  and  $\beta$ . Since volume fractions of all components add up to 1 in both phases, for each phase

$$\phi_1^\alpha + \phi_2^\alpha + \phi_3^\alpha = 1 \quad (6)$$

$$\phi_1^\beta + \phi_2^\beta + \phi_3^\beta = 1 \quad (7)$$

Equations 2-7 describe the compositions of the equilibrium phases. Given interaction parameters and molar volumes, these equations were used to compute the binodal of the water-2-propanol-EVAL system in this report. Procedures for calculations of binodals have been described by Altena,<sup>8</sup> McHugh,<sup>9</sup> and Cheng.<sup>10</sup> For our calculations, we preferred the computation method presented by Cheng et al.<sup>10</sup>

**Crystallization Equilibrium.** As an equilibrium is established between the liquid phase and the polymer crystal in a ternary system, Cheng has derived an equation for the crystallization equilibrium.<sup>10</sup>

$$\begin{aligned} \frac{1}{RT} \left[ C \left( 1 - \frac{T}{T_m} \right) - AT \ln \frac{T}{T_m} - \frac{B}{2} (T^2 - TT_m) \right] + \\ \frac{V_u}{V_3} \ln \phi_3 + \frac{V_u}{V_3} (1 - \phi_3) - \frac{V_u}{V_1} \phi_1 - \frac{V_u}{V_2} \phi_2 + \\ \left( \frac{V_u}{V_1} \phi_1 \chi_{13} + \frac{V_u}{V_2} \phi_2 \chi_{23} \right) (\phi_1 + \phi_2) - \\ \frac{V_u}{V_1} \phi_1 \phi_2 \chi_{12} - \frac{V_u}{V_1} \phi_1 \phi_2 \phi_3 \frac{\partial\chi_{13}}{\partial\phi_2} - \frac{V_u}{V_2} \phi_2^2 \phi_3 \frac{\partial\chi_{23}}{\partial\phi_2} + \\ \left( \frac{V_u}{V_1} \phi_1 \frac{\partial\chi_{13}}{\partial\phi_3} + \frac{V_u}{V_2} \phi_2 \frac{\partial\chi_{23}}{\partial\phi_3} \right) \phi_3 (\phi_1 + \phi_2) - \frac{V_u}{V_1} \phi_1 \phi_2 \phi_3 \frac{\partial\chi_T}{\partial\phi_2} + \\ \frac{V_u}{V_1} \phi_1 \phi_2 \phi_3 (\phi_1 + \phi_2) \frac{\partial\chi_T}{\partial\phi_3} + \frac{V_u}{V_1} \chi_T \phi_1 \phi_2 (1 - 2\phi_3) = 0 \quad (8) \end{aligned}$$

where  $V_u$  is the volume of polymer per mole repeating unit. The parameters  $A$ ,  $B$ , and  $C$  are related to the heat of fusion of the polymer ( $\Delta H_f$ ) and the heat capacities of the polymer in the solid ( $C_c$ ) and melt ( $C_m$ ) states. If  $C_c$  and  $C_m$  can be assumed to be linear functions of temperature, namely  $C_m = a + bT$  and  $C_c = c + dT$ , then one obtains  $A = a - c$ ,  $B = b - d$ , and  $C = \Delta H_f - AT_m - BT_m/2$ . Given the values of the interaction parameters, eq 8 can be solved to obtain the crystallization equilibrium line.

**Interaction Parameters.** The binary interaction parameter between component water and 2-propanol,  $\chi_{12}$ , is calculated from literature data on the excess Gibbs energy of mixing ( $G^E$ ), obtained from vapor pressure experiments.<sup>11</sup> Assuming that  $\chi_{12}$  has the functional form suggested by Koningsveld and Kleintjens,<sup>12</sup> parameters  $a$ ,  $b$ , and  $c$  in eq 9 can be found by least squares regression.

$$\chi_{12} = a - \frac{b}{1 - c\phi_2} \quad (9)$$

For a ternary system, following Yilmaz and McHugh,<sup>9</sup>  $\chi_{12}$  is assumed to be a function only of  $\phi_2/(\phi_1 + \phi_2)$ . Thus,  $\chi_{12}$  is obtained by replacing  $\phi_2$  with  $h_2 = \phi_2/(\phi_1 + \phi_2)$  in eq 9.

Binary interaction parameters between nonsolvent and polymer,  $\chi_{13}$  and  $\chi_{23}$ , are considered as concentration independent.  $\chi_{13}$  and  $\chi_{23}$  may be determined using data from equilibrium sorption experiments.<sup>13</sup> The following equation is employed:

$$\ln \frac{p}{p^0} = \ln \phi_i + \left( 1 - \frac{1}{x_n} \right) \phi_3 + \chi_{i3} \phi_3^2 \quad i = 1 \text{ or } 2 \quad (10)$$

where  $p^0$  is the saturation pressure of the nonsolvent.  $x_n$  is the degree of polymerization of the polymer. As both liquids are separately nonsolvents for the polymer

at the experimental temperature, it is impossible to determine that  $\chi_{13}$  and  $\chi_{23}$  estimated from this method were concentration dependent.

Experimental data for the ternary interaction parameter,  $\chi_T$ , of the system water–2-propanol–EVAL are not available in the literature. In this study, we simply treat  $\chi_T$  as an empirical correction parameter. A fitting procedure was performed by systematically varying  $\chi_T$  to see if both the liquid–liquid phase equilibrium and the crystallization equilibrium fit the experimental data. A reasonable agreement between theoretically predicted and experimentally obtained data will be shown in this study, but it cannot be obtained by simply using binodal interaction parameters only.

## Experimental Section

**Material.** Polymer solutions were prepared using EVAL polymer (105A, Kuraray Co. Ltd., Japan) having an average molecular weight  $M_w = 56,000$  g/mole (intrinsic viscosity = 0.87 dl/g),<sup>14</sup> and an average ethylene content of 44 mole %. LC-grade 2-propanol (Alps Chem, Taiwan) was used as received. Water was deionized and double distilled before use.

**Methods: Liquid–liquid Demixing and Crystallization-Induced Gelation Boundaries.** The liquid–liquid demixing and crystallization-induced gelation boundaries were determined by the cloud point method described in a previous publication.<sup>14</sup> A specific amount of EVAL polymer (dried in an oven at 50 °C) was mixed with a suitable amount of water–2-propanol mixture and sealed in a Teflon-lined bottle (20 mL). This mixture was mechanically agitated at 70 °C until a clear homogeneous solution was obtained. The solution was then placed in an isothermal thermostat maintained at 60 °C for a period of 2 weeks. With different compositions, three types of phase-separated results may be observed: (i) the solution precipitates into a translucent or a white solid gel; (ii) the solution undergoes liquid–liquid phase separation into two clear liquid phases; (iii) following case (ii), the solution then becomes a clear liquid phase coexisting with a white solid. The equilibrium gelation point (case i) was identified as the composition at which a sharp increase in turbidity was observed by a turbidity bridge (Digital turbidimeter, Orbeco-Hellige). For case ii, the location of the binodal in the ternary phase diagram was determined and no other phase transition interfered with the liquid–liquid demixing process. The weight of two liquid phases was determined by aspirating the dilute phase, taking care not to remove the layer of the concentrated phase. The composition of the dilute phase, which contained essentially only water and 2-propanol, was determined by gas chromatography (China Chromatography, 8700T). Knowing the overall composition, allowed us to calculate the tie line compositions. For case iii, gelation occurs in the polymer-rich phase after the liquid–liquid demixing. Therefore, the location of the liquid–liquid miscibility gap and gelation region will overlap in the phase diagram.

### Characterization of EVAL Solutions and Gels by DSC.

The thermal properties of the equilibrium EVAL solutions and gels were studied using a differential scanning calorimeter (DSC) (DuPont 2200) for the temperature range of 30 °C to the melting points of the gels at a rate of 10 °C/min.

**Equilibrium Absorption of Water and 2-Propanol of EVAL.** EVAL pellets were fused in a mechanical press at 6000 psi and 185 °C. The EVAL melt was subsequently quenched in liquid nitrogen to form EVAL films. The equilibrium absorption of water and 2-propanol of EVAL films was measured by a Cahn counterbalance at 60 °C.

## Results and Discussion

**Experimental Phase Behavior of Water–2-Propanol–EVAL.** In Figure 1, liquid–liquid demixing and gelation boundaries from cloud point measurements at 60 °C as shown. The weight fractions have been converted to volume fractions using the following values

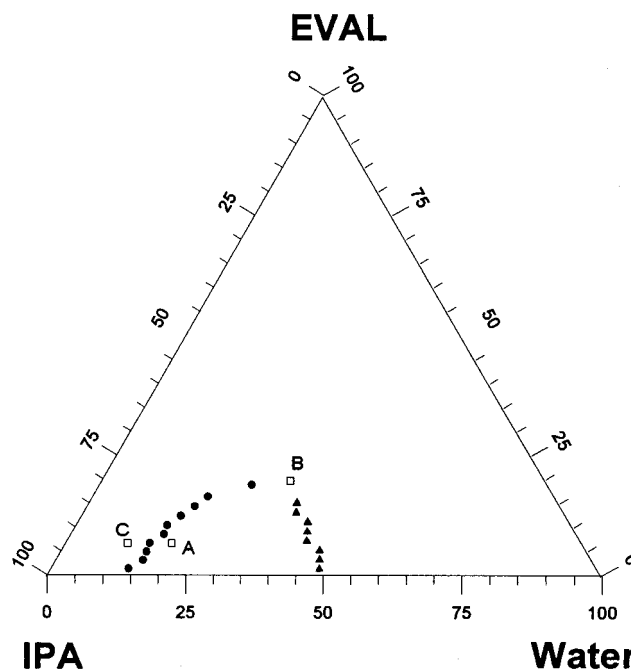


**Figure 1.** Phase diagrams of water–2-propanol–EVAL at 60 °C. The data points, denoted by filled triangles (▲) and circles (●), represent the composition at which the two liquid phases and gelation first occur in a series of samples with increasing EVAL concentration. □: dope solutions for DSC scan.

for the density: water, 0.98 g/cm<sup>3</sup>; 2-propanol, 0.755 g/cm<sup>3</sup>; EVAL, 1.14 g/cm<sup>3</sup>.<sup>15</sup> The data points, denoted by filled triangles and circles, represent the composition at which two equilibrium liquid phases (▲) and gelation (●) first occur in a series of samples with increasing EVAL concentration, respectively. A composition below these data is a homogeneous and transparent solution; i.e., EVAL is dissolved in such a cosolvent at lower polymer compositions to form a good solution. As water or 2-propanol is added to this solution to a greater extent, the water–2-propanol mixture reduces the solvation character of the EVAL polymer and acts as a nonsolvent. When the solution is beyond the gelation boundary ( $\phi_2 > 0.85$  or  $\phi_3 > 0.23$ ), the solution becomes an opaque pasty gel. In Figure 2, DSC thermograms are shown for a solution (point A in Figure 1) and two equilibrium gels (points B and C in Figure 1). The endotherms show that the melting temperature of point A is 49 °C, which is consistent with the location of A within the 60 °C gel boundary. The melting temperatures of B and C, which are beyond the 60 °C gel boundary, are higher than 60 °C. These broad melting peaks correspond to the melting of crystallites of EVAL polymer in the gel. Therefore, the gelation boundary represents the compositions of the liquid phases that coexist in equilibrium with pure EVAL. Any composition beyond this gelation boundary appears in the form of a gel induced by crystalline EVAL dispersing uniformly in the liquid phase. The differences in location between the two liquid equilibrium phases and crystallization boundaries are large. The binodal boundary is located at the right part of the phase diagram. In order to investigate the unexpected phenomenon, the phase behavior of the water–2-propanol–EVAL ternary system was determined theoretically.

**Calculation of the Phase Behavior of Water–2-Propanol–EVAL for Constant  $\chi_T$ .** The calculated binodals determined by solving eq 2–7 are shown in

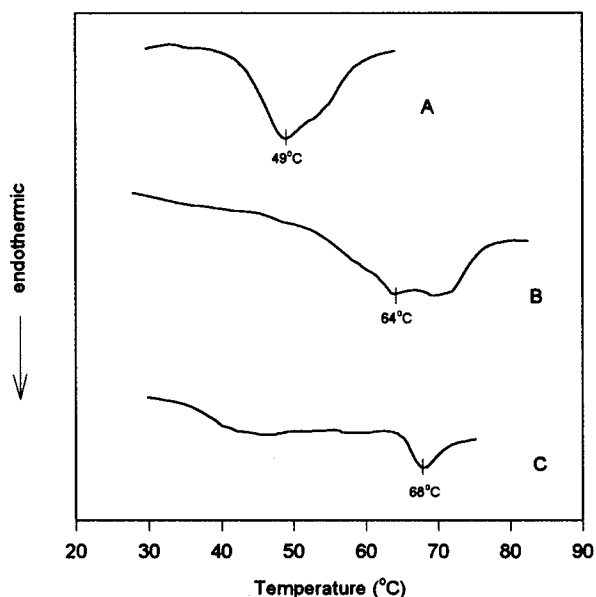


**Figure 2.** DSC thermograms of crystalline EVAL gels from 30 °C to the melting points of the gels at a rate of 10 °C/min. Curves A–C represent respectively gel points A–C in Figure 1.

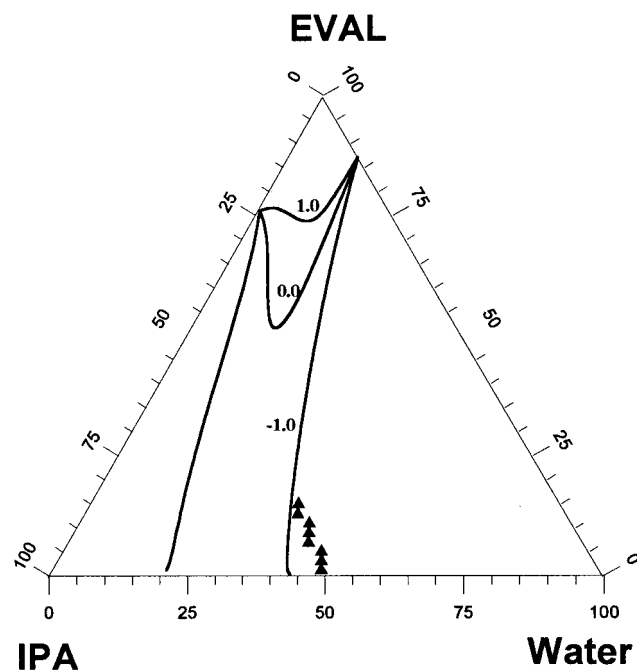


**Figure 3.** Comparison between theoretically calculated binodals and experimentally determined liquid-liquid demixing data points (denoted by filled triangular symbols, ▲). Solid lines represent calculated binodal boundaries for  $\chi_T = 1, 0$ , and  $-1$ . Numbers indicate the value of  $\chi_T$  used for the calculations.

Figure 3 with the experimental liquid-liquid demixing data points (denoted by triangular symbols, ▲). The physical constants for EVAL employed in binodal computations are given in Table 1.<sup>14</sup> The concentration-dependent interaction parameter for the water-2-propanol binary pair,  $\chi_{12}$ , was determined separately using vapor-liquid equilibrium data from the literature.<sup>11</sup> Nonlinear regression was then used with eq 9 to find the parameters  $a$ ,  $b$ , and  $c$ , and the results are given in Table 2. The values of  $\chi_{13}$  and  $\chi_{23}$  were found to be 1.58 and 1.17, respectively, by using eq 10 from the equilibrium absorption of water and 2-propanol of

**Table 1.** Physical Constants for the EVAL Polymer<sup>a,14</sup>

$T_m$ (°C)	$C_m$ [J/(mol K)]	$C_c$ [J/(mol K)]	$\Delta H_f$ (kJ/kg)	$\rho$ (g/cm <sup>3</sup> )	$M$
163.1	0.0405T+87.543	0.4749T-83.59	68.62	1.14	56 000

<sup>a</sup>  $T_m$ , melting temperature;  $C_m$ , melt heat capacity;  $C_c$ , solid heat capacity;  $\Delta H_f$ , enthalpy of fusion;  $\rho$ , density;  $M$ , molecular weight.

**Table 2.** Summary of Interaction Parameter Data

binary system	interaction parameter, $\chi_{ij}$
water (1)–2-propanol (2)	$0.6895 + 0.3894/(1.0 - 0.7214h_2)^a$
water (1)–EVAL (3)	1.58
2-propanol (2)–EVAL (3)	1.17

<sup>a</sup>  $h_2 = \phi_2/(\phi_1 + \phi_2)$ .

EVAL at 60 °C. These large positive values are consistent with the fact that water and 2-propanol are separately a nonsolvent for EVAL.

The value of  $\chi_T$  is zero for the initial analysis, which means the ternary interaction parameter is neglected. As shown in Figure 3, the binary interaction parameters summarized in Table 2 cannot be used to properly describe the experimental binodal boundary of the system. The result is relatively unsatisfactory and it predicts that no cosolvency can be obtained at low polymer concentrations ( $\phi_3 < 0.55$ ). For a theoretical consideration, it was further attempted to see if it would be possible to fit the experimental data by using a  $\chi_T$  parameter as an adjustable fitting parameter. The main difficulty in applying the  $\chi_T$  parameter to this cosolvent system is to measure the  $\chi_T$  parameter directly. For simplicity, the phase diagram of water-2-propanol-EVAL at 60 °C was calculated by selecting values of  $\chi_T = 1$  and  $-1$  to ascertain whether or not  $\chi_T$  is a significant factor.

Figure 3 shows no improvement for cosolvency and a poor agreement with the experimental data points for  $\chi_T = 1$ . When compared to the result for  $\chi_T = 0$  the liquid-liquid demixing region below the binodal boundary is enlarged to more near the polymer apex. However, the effect of  $\chi_T$  on the liquid-liquid miscibility gap is significant for  $\chi_T = -1$ . Calculation of the solubility behavior of mixtures indicates that the one-phase region occurs between two binodal boundaries. The polymer will dissolve in compositions between  $\phi_1 = 0.2$  and 0.45. On the other hand, the crystallization equilibrium line at 60 °C was determined with eq 8 and the result was also compared with experimental gelation data (Figure 4). The heat of fusion at the melting temperature and the heat capacities for EVAL polymer in the solid and melt states are given in Table 1.<sup>14</sup> The difference of the crystallization equilibrium line for  $\chi_T = 0$  and  $\chi_T = 1$  is not significant. The crystallization equilibrium line is almost a straight line in the phase diagram. Gelation will occur when the composition is above this crystallization equilibrium line. However, for  $\chi_T = -1$ , the crystallization equilibrium line bends to the water-2-propanol axis at the right part of the phase diagram and a better fit with experimental data points is obtained. When the binodal and crystallization boundaries for  $\chi_T = -1$  are combined, the phenomenon of cosolvency will be located below the crystallization equilibrium curve and between the two binodal boundaries. At higher polymer concentrations ( $\phi_3 > 0.23$ ), crystallization processes take over the cosolvency. It is clear that the experimentally found trends are appropriately predicted for  $\chi_T = -1$ .

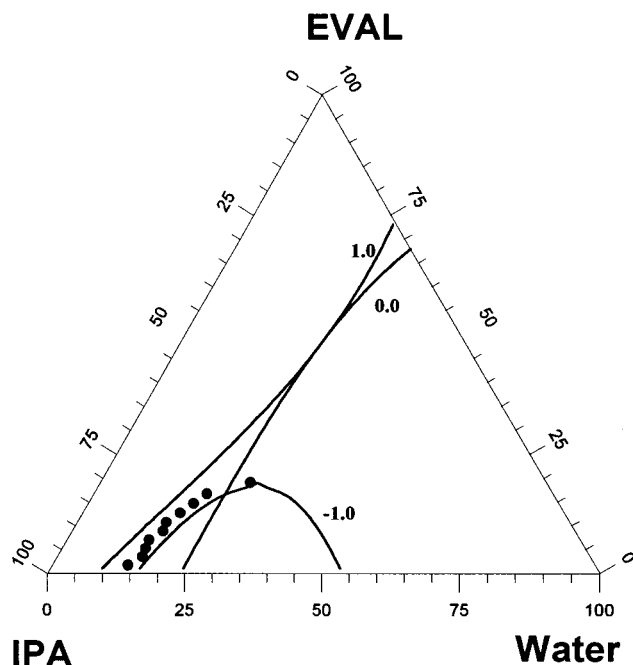


**Figure 4.** Comparison between theoretically calculated crystallization equilibrium curves and measured gel points (denoted by filled circles, ●). Solid lines represent calculated crystallization equilibrium lines for  $\chi_T = 1, 0$  and  $-1$ . Numbers indicate the value of  $\chi_T$  used for the calculations.

**Calculation of Phase Behavior of Water–2-Propanol–EVAL for Concentration-Dependent  $\chi_T$ .** Since  $\chi_T$  should probably vary with solvent composition and this could alter the phase behavior considerably, a concentration-dependent ternary interaction parameter is proposed. Although the  $\chi_T$  value cannot be measured experimentally, an approximate form can be derived if some assumptions are made. We considered a three-parameter rational form given by

$$\chi_T = a + b\phi_2 + c\phi_3 \quad (11)$$

where  $a$ ,  $b$ , and  $c$  are empirical coefficients. Since the concentration of polymer or nonsolvent has an adverse effect on the cosolvency,  $b$  and  $c$  are assumed to be greater than zero. In addition,  $a$  is assumed to be less than zero following the above mentioned result.

A trial-and-error procedure was used to obtain the concentration-dependent  $\chi_T$ , in which experimental data points on the binodal boundary were fitted. The best fit is obtained by using  $\chi_T = -1.7 + 0.5\phi_2 + 1.0\phi_3$ . Figure 5 shows that the computed binodal boundary and tie lines match closely the experimental data points, suggesting that a reliable curve fitting has been obtained. This concentration-dependent  $\phi_T$  was then used with eq 8 to calculate the crystallization equilibrium curve. Figure 5 shows that in this case the crystallization equilibrium curve agrees well with the experimental data points. These agreements are the result of the fitting procedure where  $\chi_T$  has been used as a concentration-dependent parameter. In addition, the data points at the water–EVAL axis and the 2-propanol–EVAL axis (denoted by square symbols, ■) depict the measured equilibrium absorption of water and 2-propanol of EVAL at 60 °C. The calculated results, points S and T, perfectly fit the experimental data points. This further assures a reliable calculation.

Overall, the thermodynamic description of this cosolvent system in terms of the interaction parameters is

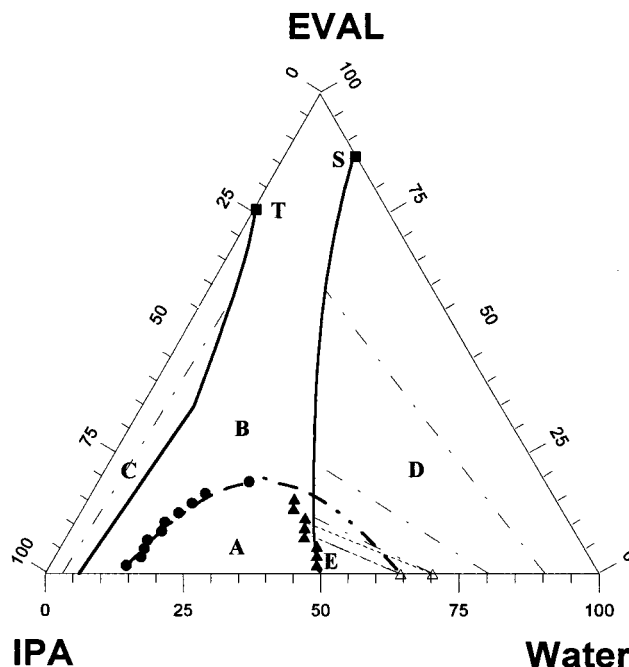


**Figure 5.** Comparison between theoretically calculated phase behavior using  $\chi_T = -1.7 + 0.5\phi_2 + 1.0\phi_3$  and experimentally determined phase transition: (▲) measured points of polymer-rich phase; (Δ) measured points of polymer-poor phase; (●) measured gel points; (■) equilibrium absorption data; (—) computed binodal; (---) computed crystallization equilibrium line; (---) computed tie line; (---) measured tie line.)

complicated by the inability to determine  $\chi_T$  directly, but one could attempt to estimate the value of  $\chi_T$  by using a numerical method to obtain the best fitted result from the limited experimental data. Therefore, unknown phase boundaries that could not be obtained experimentally can be calculated. Figure 5 shows the binodal and crystallization boundaries divide the phase diagram into five parts. Any solution in the region A is single-phase and homogeneous. Region B, defined above the crystallization curve, is metastable with respect to pure EVAL. Any composition in this region will precipitate into a gel induced by crystallization. Regions C and D, within the binodal phase envelope, are metastable with respect to both liquid–liquid phase separation and crystallization. Actually, Figure 5 represents two phase diagrams, one approximates true equilibrium between the EVAL solution and EVAL crystals and the other represents liquid–liquid demixing of the supercooled liquid. Hence, the phases that are drawn together in Figure 5 for simplicity cannot really exist together.<sup>16</sup> In general, initiation of liquid–liquid demixing is more rapid than nucleation of polymer crystallization, which requires a rearrangement of polymer,<sup>17,18</sup> so liquid–liquid demixing is kinetically favored to separate the supercooled solution, in which crystal growth does not occur, into two clear liquid phases. Subsequently, the polymer-rich phase will always be supersaturated with respect to crystallization; thus, EVAL polymers eventually crystallize to form a white gel solid to coexist with a clear liquid phase in region D. Conversely, if crystallization has occurred at a large supersaturation, then this solution could not undergo a further phase separation. Consequently, no liquid–liquid demixing could be obtained experimentally in region C. In addition, it is interesting to notice that the crystallization equilibrium curve intersects the binodal boundary at region E. In contrast to regions C

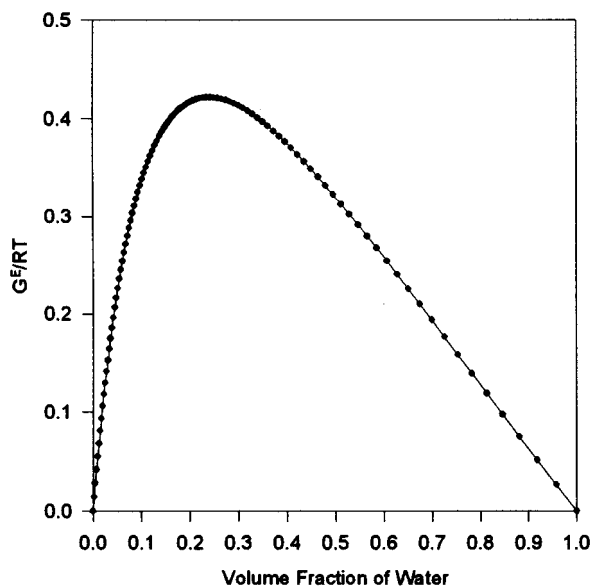


**Figure 6.** Excess free energy of mixing ( $G^E/RT$ ), calculated from vapor pressure data,<sup>11</sup> for the binary liquid system water and 2-propanol.

and D, pure liquid–liquid demixing was observed at region E. This suggests that the location of the binodal in the ternary phase diagram can be observed experimentally and no other phase transition interfered with the liquid–liquid demixing process. Accordingly, the location of the liquid–liquid miscibility gap and crystallization region does not overlap in this region.

**Mechanism of Cosolvency.** The values of  $\chi_{12}$  and  $\chi_{13}$ , estimated from equilibrium sorption experiments, appear to be relatively high for nonsolvent–polymer interaction. However, EVAL is found to be soluble in water–2-propanol mixtures. The existence of this cosolvent system clearly indicates that only binary interaction parameters approach the problem of inadequate cosolvency. Therefore, one might attempt to rationalize this behavior by postulating the existence of a ternary interaction parameter,  $\chi_T$ . In this study, although the  $\chi_T$  value is only an estimate, the results indicate that  $\chi_T$  cannot be neglected and might even dominate the calculated phase behavior to coincide with the experimental data. The best-fitted  $\chi_T$  is negative (from  $-0.7$  to  $-1.7$ ) for all compositions. This suggests a strong affinity between the polymer and the cosolvent mixtures. On such a basis, a mechanism for cosolvency can be proposed: this system favors the formation of (1–2–3) contacts (1–2), (1–3), or (2–3) contacts.<sup>19</sup>

In a pure nonsolvent, the nonsolvent–polymer contacts are energetically unfavorable and the polymer cannot dissolve. Addition of another nonsolvent to this solution leads to the formation of increasing numbers of (1–2) contacts by forming a complex by intermolecular hydrogen bonding in the solution. Analysis of existing vapor pressure data for the binary liquid system water and 2-propanol<sup>11</sup> shows that the excess free energy of mixing ( $G^E/RT$ ) is positive (Figure 6); i.e., (1–2) contacts are not particularly favored energetically. Therefore, in a cosolvent system, one can postulate the formation of (1–2–3) contacts on dissolution of the polymer in the solution that lowers the free energy of the system. This explanation is consistent with the EVAL polymer being soluble in the composition range  $\phi_1 = 0.15$ – $0.50$  (Figure 5); in a similar composition, the excess mixing free energy of the water–2-propanol

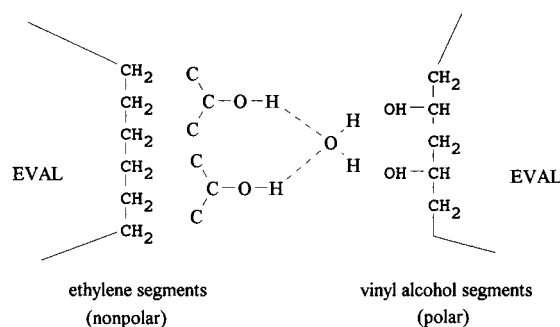


**Figure 7.** Schematic representation of the cosolvency mechanism of the EVAL polymer in the water–2-propanol mixture. The polar groups of water and 2-propanol may tend to associate with each other and present a nonpolar environment in which the ethylene segments of the polymer can dissolve. On the other hand, the vinyl alcohol segments of the polymer may interact with the polar groups exposed on the 2-propanol–water complex.

system has larger values (e.g.,  $G^E/RT > 0.3$ ) for the water fraction being between 0.1 and 0.5.

One probably considers that the so-called (1–2–3) contact is a polymer chain and its immediate solvent environment as a whole rather than necessarily depicting isolated contacts involving a segment of each of the three species. Figure 7 is a schematic representation of the cosolvency mechanism of the EVAL polymer in the water–2-propanol mixture: the polar groups of water and 2-propanol may associate with each other to present a nonpolar environment in which the ethylene segments of the polymer can dissolve. On the other hand, the vinyl alcohol segments of the polymer may interact with the polar groups exposed on the 2-propanol–water complex. Therefore, the formation of (1–2–3) contacts will pull the polymer into solution and the cosolvent action can be explained qualitatively such that the introduction of a polymer chain into the binary solvent environment serves to bind the water–2-propanol complex more strongly. Cosolvency is then a consequence of the polymer maintaining the optimum solvent environment, which will ensure maximum compatibility among the species. The implication is that the existence of a  $\chi_T$  parameter would improve the fit, but it is difficult to determine the value of  $\chi_T$  from an experimental measurement.

Overall, dissolution of the polymer will occur when a sufficient number of (1–2) contacts have formed in the vicinity of a polymer chain to allow it to be drawn into solution by the formation of sufficient (1–2–3) contacts.<sup>20</sup> This leads to the observed phase behavior that polymer dissolves in a range of mixtures of two liquids. As neither (1–3) nor (2–3) contacts are energetically favorable, any alteration in the solvent composition that increases either component 1 or component 2 in the mixture will destroy the stability of (1–2–3) contacts. In addition, such a change will reduce the (1–2) contacts and there will be more (1–1) and (2–2) contacts than the polymer can tolerate. When the system can no longer maintain sufficient (1–2–3) contacts, phase separation takes place. Furthermore, since the EVAL polymer can crystallize in the water–2-propanol mixture, the cosolvency phenomenon will be limited at lower polymer concentrations. While this might provide a simple explanation for the behavior of the present system, it is a useful starting point to explain that the  $\chi_T$  parameter plays a major role in determining whether cosolvency will be observed.

## Conclusion

The cosolvent system water–2-propanol–EVAL was studied at 60 °C. The polymer was soluble in liquid mixtures in the composition range  $\phi_1 = 0.15$ – $0.50$ , the maximum polymer solubility ( $\phi_3 = 0.23$ ) occurring at  $\phi_1 = 0.40$ . The above discussion indicates that the ternary interaction parameter cannot be neglected when the thermodynamic equilibrium properties of the system water–2-propanol–EVAL are described by the Flory–Huggins theory. The sign and magnitude of  $\chi_T$  can be considered as a guide to possible cosolvency; when  $\chi_T$  is negative, the nonsolvent–nonsolvent mixtures may act as a cosolvent for the polymer. However, the nonsolvent–nonsolvent mixtures are unlikely to dissolve the polymer if  $\chi_T$  is positive. In addition, the optimum fit to the experimental data can be obtained by choosing the value of  $\chi_T$  is  $-1.7 + 0.5\phi_2 + 1.0\phi_3$ . The mechanism of cosolvency is then discussed in relation to  $\chi_T$  and the excess mixing free energy of the two liquid components. The major weakness is that the theory fails to predict the  $\chi_T$  value directly. In order to study systematically the phase behavior of a ternary system it is necessary to measure the  $\chi_T$  value directly and correctly; therefore, further investigation is in progress to measure the value of  $\chi_T$  in our laboratory.

**Acknowledgment.** The authors thank the National Science Council of the Republic of China for their financial support of project NSC 86-2216-E-002-003.

## References and Notes

- (1) Miles, F. D. *Cellulose nitrate*; Imperial Chemical Industries Ltd., Oliver and Boyd: Edinburgh, London, 1955; Chapter V.
- (2) Katime, I.; Ochoa, J. R. *Eur. Polym. J.* **1984**, *20*, 99.
- (3) Li, S. G. Preparation of hollow fiber membranes for gas separation. Ph.D. Dissertation, University of Twente, the Netherlands, 1994.
- (4) Horta, A.; Gargallo, L.; Radic, D. *Macromolecules* **1990**, *23*, 5320.
- (5) Campos, A.; Gavara, R.; Tejero, R.; Gomez, C.; Celda, B. J. *Polym. Sci., Polym. Phys. Ed.* **1989**, *27*, 1599.
- (6) Pouchly, J.; Zivny, A.; Solc, K. *J. Polym. Sci., Part C* **1968**, *23*, 245.
- (7) Van de Witte, P.; Dijkstra, P. J.; Van de Berg, J.W.A.; Feijen, J. *J. Polym. Sci., Polym. Phys.* **1996**, *34*, 2553.
- (8) Altena, F. W.; Smolders, C. A. *Macromolecules* **1982**, *15*, 1491.
- (9) Yilmaz, L.; McHugh, A. J. *J. Appl. Polym. Sci.* **1986**, *31*, 997.
- (10) Cheng, L. P.; Dwan, A. W.; Gryte, C. C. *J. Polym. Sci., Polym. Phys.* **1994**, *32*, 1183.
- (11) Gmehling, J.; Onken, U.; Arlt, W. *Vapor-Liquid Equilibrium Data Collection Aqueous Organic Systems (supplement 1)*; Dechema Chemistry Data Series; Dechema, New York, 1977, Vol. I, Part 1a, p 327.
- (12) Koningsveld, R.; Kleintjens, L. A. *Macromolecules* **1971**, *4*, 637.
- (13) Bonner, D. J. *Macromol. Sci.-Rev. Macromol. Chem.* **1975**, *13*, 263.
- (14) Young, T. H.; Lai, J. Y.; Yu, W. M.; Cheng, L. P. *J. Membr. Sci.* **1997**, *128*, 55.
- (15) Okaya, T.; Ikari, K. In *Polyvinyl alcohol-developments*; Finch, C.A., Ed.; John Wiley & Sons Ltd.: Chichester, England, 1982; p 202.
- (16) Aubert, J. H. *Macromolecules* **1988**, *21*, 3468.
- (17) Cheng, L. P.; Dwan, A. W.; Gryte, C. C. *J. Polym. Sci., Polym. Phys.* **1995**, *33*, 211.
- (18) Cheng, L. P.; Dwan, A. W.; Gryte, C. C. *J. Polym. Sci., Polym. Phys.* **1995**, *33*, 223.
- (19) Cowie, J. M. G.; McEwen, I. J. *J. Chem. Soc., Faraday Trans.* **1974**, *70*, 171.
- (20) Cowie, J. M. G.; McCrindle, J. T. *Eur. Polym. J.* **1972**, *8*, 185–1191.

MA9710388